

Supporting Information

Facet-Selective Deposition of FeO_x on α -MoO₃ Nanobelts for Lithium Storage

Yao Yao,¹ Nuo Xu,² Doudou Guan,¹ Jiantao Li,¹ Zechao Zhuang,¹ Liang Zhou,^{*,1} Changwei Shi¹, Xue Liu¹, and Liqiang Mai^{*,1}

¹State Key Laboratory of Advanced Technology for Materials Synthesis and Processing, Wuhan University of Technology, Hubei, Wuhan 430070, China

²School of Chemistry, Chemical Engineering and Life Sciences, Wuhan University of Technology, Hubei, Wuhan 430070, China

**E-mail: liangzhou@whut.edu.cn; mlq518@whut.edu.cn*

Experimental Section

Materials synthesis: α -MoO₃ nanobelts are synthesized according to a reported hydrothermal method.¹ In a typical synthesis, 10 mmol of Mo powder was dissolved in a mixture of 20 mL of 30 wt. % H₂O₂ and 20 mL of H₂O under stirring at 25 °C. The resulting solution was stirred for 12 h at 25 °C. The solution was then transferred into a Teflon-lined stainless-steel autoclave, sealed, and hydrothermally treated at 180 °C for 24 h, after which a white suspension (α -MoO₃ nanobelts) was obtained.

For the fabrication of heterostructured α -MoO₃@FeO_x nanobelts, 0.686 g (NH₄)₂Fe(SO₄)₂·6H₂O was dissolved in 40 mL H₂O. Then, the as-synthesized α -MoO₃ nanobelts (2 mL) were added dropwise into the (NH₄)₂Fe(SO₄)₂·6H₂O solution under stirring at 70 °C for 4 h to obtain the α -MoO₃@FeO_x heterostructures.

Characterization: The morphology of the as-prepared products were investigated by field-emission scanning electron microscopy (JEOL JSM-7100 F) at an acceleration voltage of 20 kV. Transmission electron microscopy (TEM), selected area electron diffraction (SAED) pattern, and high-resolution TEM (HRTEM) images were collected by a JEOL JEM-2100F. An energy-dispersive X-ray spectroscopy (EDS) facility attached to the TEM was used to analyze the element distribution. The crystal phase of products was characterized by X-ray diffraction (XRD). XRD patterns of the products were recorded by a Rigaku D/MAX-III diffractometer with monochromatized Cu K_α radiation. The chemical composition of the products was analyzed by inductively coupled plasma-atomic emission spectrometry (ICP-AES, PerkinElmer Optima 4300DV). X-ray photoelectron spectroscopy (XPS) spectra were obtained on a ESCALAB 250 system with a monochromatic Al K_α source (1,486.6 eV). All XPS profiles were calibrated based on the C 1s peak at 284.6 eV.

Electrochemical measurements: Electrochemical properties were measured in 2016 type coin cells. The coin cells were assembled in an argon-filled glovebox with lithium metal as the counter and reference electrodes. The working electrode was

fabricated by mixing 70 wt.% of the active material (α -MoO₃ and α -MoO₃@FeO_x), 20 wt.% of conductive carbon black (acetylene black), and 10 wt.% of carboxymethyl cellulose (CMC) binder in H₂O. The mass loading of the active material was ~ 1.5 mg cm⁻². The electrolyte used was a solution of 1 M LiPF₆ in ethylene carbonate, dimethyl carbonate, ethyl methyl carbonate (1:1:1 by volume). Galvanostatic discharge/charge experiments were performed in the potential range of 0.005 – 3 V with a battery testing system (LAND CT 2001A) at room temperature. Cyclic voltammetry (CV) and electrochemical impedance spectroscopy (EIS) were conducted using an autolab potentiostat galvanostat.

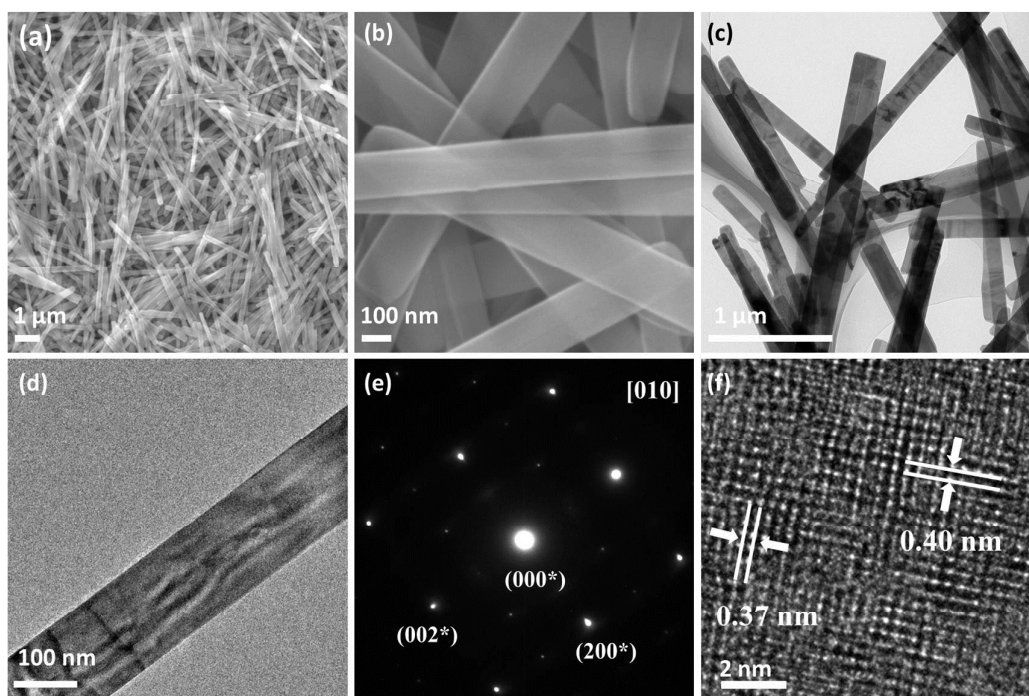


Figure S1. SEM images (a, b), TEM images (c, d), SAED pattern (e) and HRTEM image (f) of α -MoO₃ nanobelts.

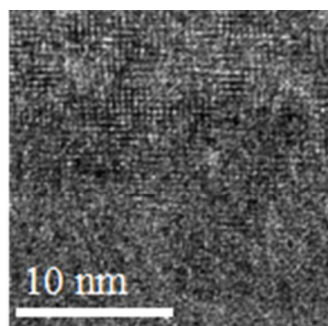


Figure S2. The HRTEM image of the interfacial region between FeO_x and MoO_3 .

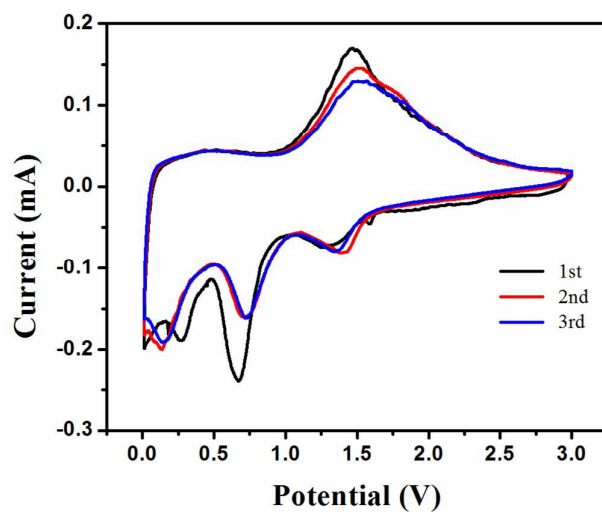


Figure S3. CV curves of $\alpha\text{-MoO}_3@ \text{FeO}_x$ at a sweep rate of 0.1 mV s^{-1} in the potential range of $0.005 - 3.0 \text{ V vs. Li/Li}^+$.

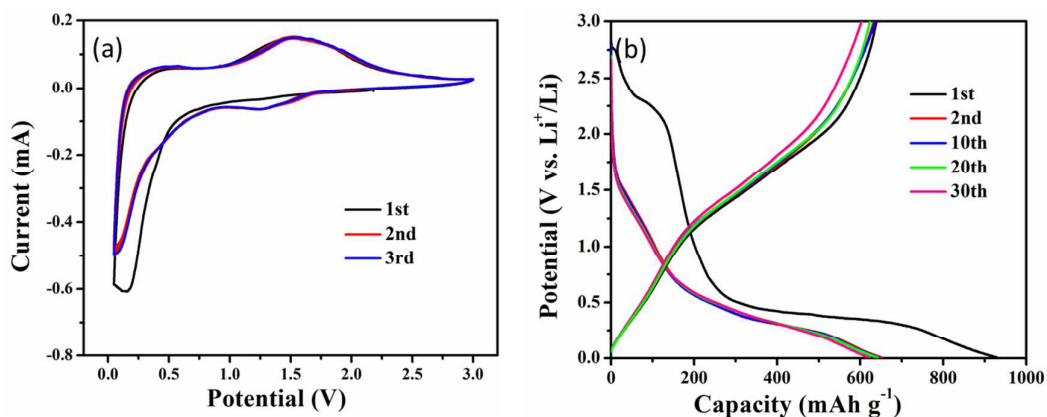


Figure S4. CV curves of α - MoO_3 at a sweep rate of 0.1 mV s^{-1} in the potential range of $0.005 - 3.0 \text{ V vs. Li/Li}^+$ (a); galvanostatic discharge-charge voltage profiles of the α - MoO_3 nanobelts at 200 mA g^{-1} (b).

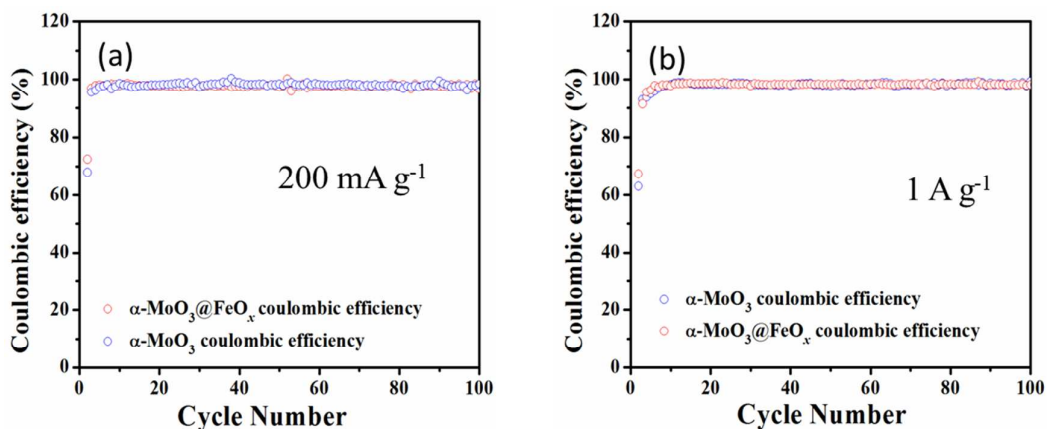


Figure S5. Coulombic efficiency of α - MoO_3 and α - $\text{MoO}_3@FeO_x$ at 200 mA g^{-1} (a) and 1 A g^{-1} (b).

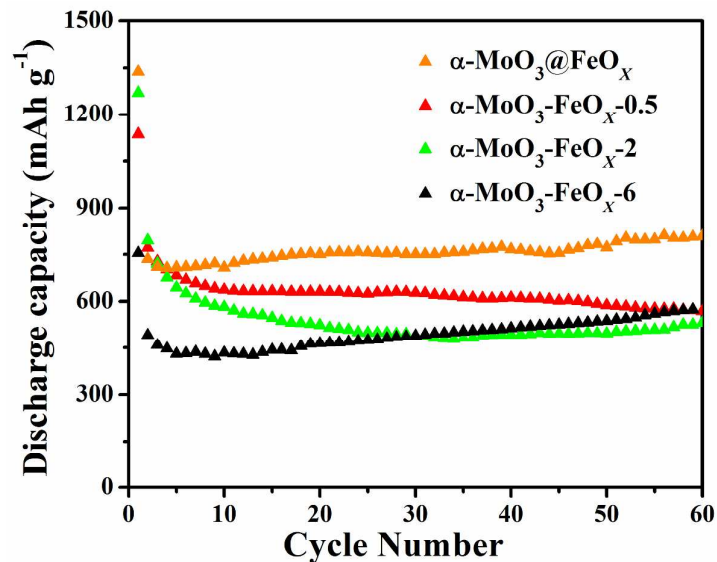


Figure S6. Comparison of cycling performances of the $\alpha\text{-MoO}_3\text{-FeO}_x\text{-0.5}$, $\alpha\text{-MoO}_3\text{-FeO}_x\text{-2.0}$, $\alpha\text{-MoO}_3\text{-FeO}_x\text{-6.0}$ and $\alpha\text{-MoO}_3\text{@FeO}_x$ nanobelts at 200 mA g^{-1} .

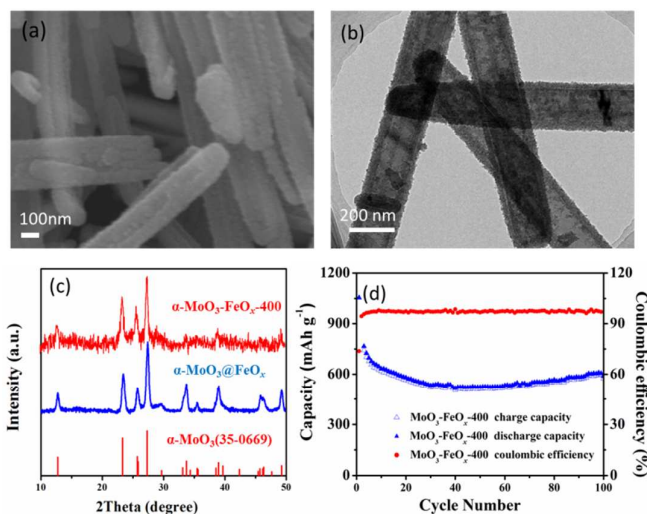


Figure S7. SEM image (a) and TEM image (b) of $\alpha\text{-MoO}_3\text{-FeO}_x\text{-400}$; XRD patterns of $\alpha\text{-MoO}_3\text{-FeO}_x\text{-400}$ and $\alpha\text{-MoO}_3\text{@FeO}_x$ (c); cycling performance of $\alpha\text{-MoO}_3\text{-FeO}_x\text{-400}$ at 200 mA g^{-1} .

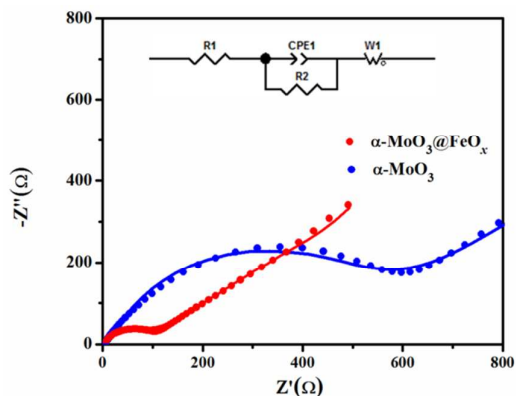


Figure S8. Nyquist plots of the α -MoO₃ and α -MoO₃@FeO_x electrodes. The inset shows the equivalent circuit. In the equivalent circuit, R1 is the total resistance of the electrolyte, separator, and electrical contacts; R2 is the Faradic charge-transfer resistance; CPE1 is the constant phase-angle element; W1 represents the Warburg impedance.

References

1. Zhou, L.; Yang, L.; Yuan, P.; Zou, J.; Wu, Y.; Yu, C., α -MoO₃ Nanobelts: A High Performance Cathode Material for Lithium Ion Batteries. *J. Phys. Chem. C* 2010, 114, 21868-21872.